"Biomarkers of tumor redox status in response to modulations of glutathione and thioredoxin antioxidant pathways."

Kengen, Julie ; Deglasse, Jean-Philippe ; Neveu, Marie-Aline ; Mignion, Lionel ; Desmet, Céline ; Gourgue, Florian ; Jonas, Jean-Christophe ; Gallez, Bernard ; Jordan, Bénédicte

Abstract

The ability of certain cancer cells to maintain a highly reduced intracellular environment is correlated with aggressiveness and drug resistance. Since the gluthathione (GSH) and thioredoxin (TRX) systems cooperate to a tight regulation of ROS in cell physiology, and to a stimulation of tumor initiation and progression, modulation of the GSH and TRX pathways are emerging as new potential targets in cancer. In vivo methods to assess changes in tumor redox status are critically needed to assess the relevance of redox-targeted agents. The current study assesses in vitro and in vivo biomarkers of tumor redox status in response to treatments targeting the GSH and TRX pathways, by comparing cytosolic and mitochondrial redox nitroxide Electron Paramagnetic Resonance (EPR) probes, and cross-validation with redox dynamic fluorescent measurement. For that purpose, the effect of the GSH modulator buthionine sulfoximine (BSO) and of the TRX reductase inhibitor auranofin were measured in vitro us...

Document type : *Article de périodique (Journal article)*

Biomarkers of tumor redox status in response to modulations of glutathione and thioredoxin antioxidant pathways

Julie Kengen*[,1], Jean-Philippe Deglasse*[,2], Marie-Aline Neveu[1], Lionel Mignion[1], Céline Desmet[1], Florian Gourgue[1] Jean-Christophe Jonas[2], Bernard Gallez[1], Bénédicte F. Jordan[1]

*authors contributed equally to this work

[1] Université catholique de Louvain (UCL), Louvain Drug Research Institute, Biomedical Magnetic Resonance Group, Avenue Mounier 73 box B1.73.08, 1200 Brussels, Belgium.

[2] Université catholique de Louvain, Institute of Experimental and Clinical Research, Pole of Endocrinology, Diabetes and Nutrition, Brussels, Belgium.

Corresponding author:

Prof. B.F. Jordan, PhD
Université catholique de Louvain (UCL),
Louvain Drug Research Institute,
Biomedical Magnetic Resonance Group,
Avenue Mounier 73 box B1.73.08, 1200 Brussels, Belgium.
benedicte.jordan@uclouvain.be

Word count: 3499

Abstract

The ability of certain cancer cells to maintain a highly reduced intracellular environment is correlated with aggressiveness and drug resistance. Since the gluthatione (GSH) and thioredoxin (TRX) systems cooperate to a tight regulation of ROS in cell physiology, and to a stimulation of tumor initiation and progression, modulation of the GSH and TRX pathways are emerging as new potential targets in cancer. In vivo methods to assess changes in tumor redox status are critically needed to assess the relevance of redox-targeted agents. The current study assesses in vitro and in vivo biomarkers of tumor redox status in response to treatments targeting the GSH and TRX pathways, by comparing cytosolic and mitochondrial redox nitroxide Electron Paramagnetic Resonance (EPR) probes, and cross-validation with redox dynamic fluorescent measurement. For that purpose, the effect of the GSH modulator buthionine sulfoximine (BSO) and of the TRX reductase inhibitor auranofin were measured in vitro using both cytosolic and mitochondrial EPR and roGFP probes in breast and cervical cancer cells. In vivo, mice bearing breast or cervical cancer xenografts were treated with the GSH or TRX modulators and monitored using the mito-TEMPO spin probe. Our data highlight the importance of using mitochondria targeted spin probes to assess changes in tumor redox status induced by redox modulators. Further in vivo validation of the mito-tempo spin probe with alternative in vivo methods should be considered, yet the spin probe used in vivo in xenografts demonstrated sensitivity to the redox status modulators.

keywords:

tumor, redox status, spin probe, roGFP, auranofin

Introduction

Cancer cells sustain a much higher level of ROS production compared to normal cells [1]. Reports have proposed that, by buffering ROS levels, cancer cells can restrict ROS within a range of concentrations that should favor tumor progression [2, 3]. The ability of certain cancer cells to maintain a highly reduced intracellular environment is therefore strongly correlated with aggressiveness and drug resistance [4, 5]. In patients, the expression levels of human antioxidant genes (HAGs) and oxidative markers were related to tumor aggressiveness and predicted poor outcome in patients with early-stage lung adenocarcinoma [6]. Also, tumor redox parameters measured by ^{62}Cu-ATSM PET determined the outcome of patients with head and neck cancer [7]. This is in line with a recent study showing that the ratio of oxidized versus reduced GSH was strongly correlated with locoregional control of HNSCC tumors [8]. Finally, analysis of 25 independent cohorts with 5910 breast cancer patients showed that overexpression of thioredoxin (Trx1) and thioredoxin reductase (TrxR1) was associated with a poor overall survival, distant metastasis-free survival and disease-free survival [9]. Other studies showed similar correlations in non-small cell lung carcinoma [10] and colorectal cancer [11].

Within the scope, modulation of the GSH and TRX pathways are potential targets in cancer. Both systems cooperate to a tight regulation of ROS in cell physiology. They were also recently shown to cooperate for cancer initiation and progression: while GSH was required for cancer initiation, it was not required for established tumors, partly due to upregulation of the TRX pathway [12]. Moreover, blocking both GSH and TRX pathways synergistically inhibited tumor growth [12].

Several anticancer agents in development target cellular redox regulation. Drugs targeting S-glutathionylation have direct anticancer effects via cell signalling pathways and inhibition of DNA repair [13]. Of these agents, NOV-002 and canfosfamide have been assessed in phase III trials but had no significant benefit with respect to standard therapies. Similarly, initial therapy with a combination of imexon and gemcitabine did not improve the outcome of metastatic pancreatic adenocarcinoma [14]. Buthionine sulfoximine (BSO) has been successfully tested in the pre-clinical setting [15,16], and in patients in combination with melphalan in a phase I studies [17, 18, 19], in line with the observation that GSH depletion enhanced alkylator sensitivity in children with recurrent neuroblastoma [20]. Disulfiram is

currently studied in various cancer types including glioblastoma [21], glioma [22], leukemia [23], and non-small cell lung cancer [24]. Finally, efforts are ongoing to release anticancer drugs preferentially in cells having high GSH content [25].

Alternatively, agents including PX-12, auranofin and motexafin gadolinium (MGd) are being developed to target thioredoxin, which is overexpressed in many human tumors. A phase-II study was conducted using PX-12 in patients with advanced pancreatic cancer. Due to the lack of significant antitumor activity and unexpectedly low baseline Trx-1 levels, PX-12 did not prove active in unselected patients [26]. Similarly, the addition of MGd to a standard 6-week course of radiation did not improve the survival of pediatric patients with newly diagnosed intrinsic pontine gliomas [27], and its combination with standard radiation therapy was ineffective in supratentorial glioblastoma multiform [28]. Auranofin is now extensively studied in the context of anticancer therapy. Preclinical studies evidenced effects in NSCLC cells and xenografts via the inhibition of the PI3K/AKT/mTOR pathway [29], in osteosarcoma metastasis [30], mesothelioma [31], and lymphoma [32], among others.

The ability to robustly measure changes in tumor redox status in vitro and in vivo is critically needed to assess the relevance of these targeted agents. Within the scope, few techniques have the potential for in vivo translation. One method is based on the redox cycle of cell-penetrating nitroxide derivatives and their electron paramagnetic resonance (EPR) or magnetic resonance imaging (MRI) detection properties [33-37] (Fig.1). In vitro studies indicate that the « EPR detectable » nitroxide radical could be converted rapidly to the « EPR silent » hydroxylamine and/or oxoammonium by different cellular compounds (e.g., free ions of transition metals, hydroxyl and hydroperoxyl radicals, ubiquinols, NAD(P)H, and ascorbate/dehydroascorbate). In turn, hydroxylamine and oxoamonium can restore the nitroxide radical. In vivo, the interaction of hydroxylamine with superoxide and/or hydrogen peroxide seems to dominate as the process that restores the nitroxide radical and its EPR/MRI contrast [35]. The aim of the current study was to identify biomarkers of tumor redox status in response to treatments targeting the GSH and thioredoxin pathways in vitro and in vivo, by comparing cytosolic and mitochondrial nitroxide EPR probes, and cross-validation with redox dynamic fluorescent measurement. For that purpose, two human tumor cell lines were tested in the presence of the GSH inhibitor BSO and the Trx inhibitor auranofin, using cytosolic and mitochondrial nitroxides EPR probes in comparison with redox-sensitive green fluorescent

protein probes. The mitochondrial nitroxide EPR probe was then assessed in vivo on tumor xenografts following administration of BSO or auranofin.

Materials and methods

Cell Lines

Human mammary adenocarcinoma (MDA-MB-231) and Human cervix squamous cell carcinoma (SiHa) cells (American Type Culture Collection [ATCC]) were grown in Dulbecco's modified Eagle's medium (DMEM, Invitrogen, Belgium) with GlutaMAX ^{tm}, D-Glucose 1g/L and sodium pyruvate supplemented with 10 % fetal bovine serum (Invitrogen, Belgium) and 1% (v/v) penicillin-streptomycin (Invitrogen, Belgium).

In vivo xenografts

Animal studies were undertaken in accordance with Belgian and Université catholique de Louvain ethical committee regulations (agreements number UCL/2010/ MD/001 and UCL/2014/MD/026).

A total of 10^7 MDA-MB-231 cells or 10^7 SiHa cells, amplified in vitro, were collected by trypsinization, washed three times with Hanks balanced salt solution and resuspended in 100 µL of Hanks balanced salt solution. Cells were then implanted by intramuscular injection in the rear legs of NMRI nude mice. After inoculation, tumors were allowed to grow up to 7 mm +/- 1 mm in diameter prior to experimentation. Mice were anesthetized by isoflurane inhalation (Forene, Abbot, England) mixed with air in a continuous flow (2 L/min). Physiological temperature was maintained using a warm water blanket connected to a circulating water bath.

Chemicals

The nitroxide probes, mito-tempo and tempol were purchased from Sigma Aldrich (Diegem, Belgium). Solutions of the nitroxide were prepared at a stock concentration of 300 mM in saline and were then stored at -20°C before use. For in vitro experiments, nitroxide was used as a probe at a final concentration of 100 µM added just before recording of EPR spectrum. For in vivo experiments, nitroxide was used as a probe at a concentration of 6mM, mice were given one dose via intratumoral injection with a saline solution of nitroxide and EPR spectra were acquired directly after the injection.

Drug treatment

L-Buthionine-sulfoximine (BSO) and auranofin were purchased from Sigma Aldrich (Diegem, Belgium). For in vitro experiments, BSO was dissolved in saline and added to cells at a final concentration of 25 µM for 24 hours once the cells had reached 85 % confluence. Auranofin was dissolved in DMSO (Invitrogen) and added to cells at a final concentration of 5 µM for 1 hour once the cells had reached 85 % confluence. For in vivo experiments, mice were divided into 3 groups (n=5-10 mice/group). BSO group: BSO was dissolved in saline and administered 500 mg/kg by intraperitoneal injection (12.5 mg BSO/250 µl saline) in one dose 6 h before recording EPR spectrum. Auranofin group: auranofin stock solution was diluted with saline and administered 1.6 mg/kg by intraperitoneal injection in one dose 3 hours before recording EPR spectrum. Control group: mice were administered with appropriate vehicle 24h or 3h before experimentation.

In vitro EPR measurements

Cells at a density of 10^8 cells/ml were incubated with tempol (100 µM final concentration) prior to EPR measurement. The reaction mixture was transferred to a gas permeable Teflon capillary (Zeus industries, New Jersey, USA). Each capillary was then folded twice, inserted into a quartz tube open on both ends, and placed into the EPR cavity. The EPR cavity was continuously flushed at 37 °C with a gas mixture N_2/O_2 containing containing 1 % O_2. EPR spectra were recorded using a Bruker EMX EPR spectrometer operating at 9 GHz (Bruker Biospin, Germany) with typical parameters: modulation amplitude 0.25 G; Time constant 20.24 msec; Modulation frequency 100 kHz; microwave power 2.02 mW; center field 3371 G. The decay of the nitroxide EPR signal was monitored, signal intensity was recorded using a double integration of the nitroxide EPR spectra. The reduction rates of nitroxides were calculated from the initial slope.

In vitro redox dynamic fluorescent measurement

Protein thiol oxidation was measured as a marker of oxidative stress in cell lines using untargeted (cytosolic and nuclear) and mitochondria-targeted redox-sensitive green fluorescent protein (roGFP1/mt-roGFP1)[39].

Adenoviruses

The generation and amplification of adenoviruses encoding roGFP1 or mt-roGFP1 under the control of the cytomegalovirus (CMV) promoter have been described previously [40]. They were quantified using the Adeno-X Rapid Titer Kit (Clontech).

Adenoviral infection and treatments

Different types of cancer cell lines were plated on glass coverslips and cultured for 3 days in DMEM medium containing 10% FBS. Approximately 2 days before fluorescence measurements, cells were infected with Ad-roGFP1 or Ad-mt-roGFP1 at multiplicity of infection of ~100. Test substances (auranofin or BSO) were added to the culture media 1 to 24 h before the experiments.

Dynamic measurements of (mt-)roGFP1 fluorescence ratio

After culture, the coverslip was mounted in a chamber maintained at 37°C and placed on the stage of an inverted microscope equipped with a x40 objective. The cells were perfused at a flow rate of ~1 ml/min with a bicarbonate-buffered Krebs solution containing 120 mM NaCl, 4.8 mM KCl, 2.5 mM $CaCl_2$, 24 mM $NaHCO_3$, 1 g/l BSA (Fraction V, Roche) and 10 mM glucose. This solution was continuously gazed with O_2/CO_2 (94/6) to maintain pH at ~7.4. The fluorescence ratio of (mt-)roGFP1 was measured every 30 s (λexc 400/480 nm, λem 535 nm). The data were then normalized to the fluorescence ratio of the maximally reduced (set to 0%) and maximally oxidized (set to 100%) probe, as measured at the end of each experiment in the presence of 10 mM DTT then of 100 µM aldrithiol [41].

Measurement of intracellular GSH

The glutathione content of the samples was determined using the Tietze enzyme recycling assay [42] with slight modifications [43]. The two cell lines: MDA-MB-231 and SiHa were treated with BSO (25 µmol/L, 24h) or auranofin (5 µmol/L, 1h). Cells were then washed twice with ice-cold PBS and then lysed with a solution of 5-sulfosalicylic acid (5%). After two freeze-thaw cycles, samples were centrifuged at 10.000 g for 10 minutes and the resulting supernatants were kept at -80°C. Ten microliters of the samples were then placed in a mixture containing 0.2 U/ml of glutathione reductase, 50 µg/ml 5,5'-dithio-bis(2-nitrobenzoic acid), and 1 mmol/L EDTA at pH 7. The reaction was initiated by the addition of 50 µmol/L NADPH, and changes in absorbance were recorded at 412 nm. Glutathione and oxidized glutathione were distinguished by the addition of methyl-2-vinylpyridine, and their concentrations were

determined from appropriate standard curves. All glutathione determinations were normalized to the protein content of whole samples using the Pierce method.

In vitro Total Antioxidant Capacity assay

The total antioxidant capacity (TAC) in cells was analysed using the oxiselect Total Antioxidant Capacity assay kit (cell Biolabs Inc.), per manufacturer's instructions. The samples were then analysed photometrically at 490 nm using the microplate reader "SpectraMax M2" (Molecular Devices, UK).

In vivo EPR measurements

50µl of Mito-tempo (6mM in PBS) were administered by intratumoral injection to MDA-MB-231 or SiHa tumor bearing mice when the mean tumor diameter reached a size of 7+/-1mm. EPR spectra were recorded using a 1.15-GHz EPR spectrometer (ClinEPR, Lyme, NH). Measurements were performed with the following parameters: amplitude modulation 0.37 G; frequency modulation 21.3 kHz; time constant 5 msec; power 6.31 mW; scan range 50 G; center field 413 G; scan time 3 sec; 1024 points/scan, accumulation of 3 scans/measurement. The first spectrum was recorded 2 minutes after the intratumoral injection of the nitroxide. Then, spectra were recorded every 30 seconds. The decay of the nitroxide EPR signal was monitored, signal intensity was recorded using a double integration of the nitroxide EPR spectra. The reduction rates of nitroxides were calculated from the initial slope. Only tumors with a spin probe signal to noise ratio ≥ 3 and with a linear fit involving more than 5 experimental data points and a R^2 >0.75 were exploited.

Statistics

All results are expressed as mean ± standard error of the mean (SEM). ANOVA and Dunnett's multiple comparison post-test, t-test were performed to assess the statistical significance between the different groups and timings. Statistical significance was considered at the $p<0.05$ level. Graph symbols represent the following p values: * $p<0.05$, ** $p<0.01$, *** $p<0.001$.

Results

Assessment of target inhibition

To validate inhibition of the targets after administration of BSO or auranofin, glutathione dosage and 'total antioxidant capacity' assays were performed. After treatment with BSO, GSH decreased by 90 % in MDA-MB-231 and by 71% in SiHa cell lines (Fig.2 A&B; $p<0.001$, Dunnett's multiple comparison test) while auranofin had no significant effect on the GSH content in both cell lines. The non-specific 'total antioxidant capacity test' decreased to a lesser extent (32-42%) in both cell lines after treatment with BSO and auranofin (Fig.2 C&D; $p<0.05$ Dunnett's multiple comparison test).

In vitro assessment of tumor redox changes using cytosolic probes

As shown on Fig. 3 A&B, the reduction rate of the nitroxide cytosolic probe tempol was not modified by BSO or auranofin in MDA-MB-231 or SiHa tumor cells. In contrast, the fluorescence ratio of cytosolic redox-sensitive green fluorescent protein roGFP1 increased in response to both treatments in MDA-MB-231 cells (Fig.3C; $P<0.001$, Dunnett's multiple comparison test) and to auranofin ($P<0.001$, Dunnett's multiple comparison test) but not BSO in SiHa cells (Fig.3D).

In vitro assessment of tumor redox changes using mitochondrial probes

The reduction rate of the nitroxide mitochondrial probe mito-tempo was significantly modified by BSO and auranofin in MDA-MB-231 and in SiHa tumor cells, showing a 44 to 53% decrease in relative mito-tempo reduction rates (Fig.4 A&B). Accordingly, the normalized fluorescence ratio of mitochondrial roGFP1 (mt-roGFP1) increased 2 to 2.8-fold in response to the treatments in both cell lines (Fig.4 C&D).

In vivo assessment of tumor redox changes using mito-tempo

In vivo MDA-MB-231 and SiHa xenografts redox status were assessed after intratumoral administration of the mitochondrial nitroxide probe mito-tempo. We compared the relative mito-tempo reduction rates in tumor-bearing mice treated with BSO and auranofin. A significant decrease was observed in response to BSO in MDA-MB-231 xenografts (Fig.5A) and in response to both BSO and auranofin in SiHa tumors (Fig.5B).

To exclude any potential effect of the clearance of the probe by the blood flow on the estimation on the reduction rate, we compared the reduction rates of the nitroxide between control MDA-MB-231 tumors and normal tissue (muscles) in vivo. Since the reduction rate of mito-tempo was about two times slower in muscle than in tumor tissue (reduction rate in muscle tissue: 0.57+/-0.1 relative to control tumors, n=4), we can consider that clearance by tissue blood flow is not the major factor affecting the disappearance of the nitroxide signal.

Discussion

Contrarily to other techniques, spin probes have the potential for in vivo imaging of tumor redox status, using either EPR imaging or MRI [35, 36]. Our data highlight two important findings while assessing the modulation of tumor redox status using spin probes: (i) the importance of using mitochondria-targeted spin probes to assess changes in tumor redox status, as demonstrated in vitro in the current study, and (ii) the identification of a potential in vivo redox biomarker in response to modulators of the GSH or Trx systems. Despite the ability of the drugs to alter tumor redox status as confirmed using GSH dosage and the non-specific 'TCA' dosage kit, our data show that the cytosolic spin probe tempol did not detect changes in tumor redox status induced by the modulation of the GSH or Trx pathways in vitro, contrarily to the mitochondrial spin probe mito-tempo. The fact that the cytosol is maintained more reduced than the mitochondrial matrix in most mammalian cells might reduce the sensitivity of the detection method in the former compartment [44, 45, 46]. The mt-roGFP1 probe was also able to demonstrate the changes induced by BSO or auranofin in both cell lines under study. These in vitro results are in line with a previous study, using cytosolic and mitochondrial Grx1-roGFP2, in which the cytosol of cells with impaired GSH synthesis resisted oxidative stress, while significant oxidation was generated in the mitochondrial matrix upon BSO treatment [47].

In vivo assays using the mitochondrial spin probe mito-TEMPO detected changes induced by BSO or auranofin in SiHa xenografts and by BSO alone in MDA-MB-231 xenografts, although a similar trend was visible for the auranofin condition. Of interest, treatment with auranofin has been shown to inhibit TrxR activity, cell migration and clonogenic activity of MDA-MB-231 cells [48, 49], and to inhibit MDA-MB-231 cell proliferation [50]. The effects of auranofin on SiHa cells have not been documented yet. It would be relevant to compare antiproliferative, migration, and clonogenic effects of auranofin in both cell lines.

One limitation of the roGFP1 data after BSO treatment is that roGFP1 is more sensitive to gluthatione oxidation when total glutathione is reduced in the compartment of interest, as explained in [51], figures 8 and 9. Therefore, the increase in roGFP1 oxidation in BSO-treated cells may partly result from the 90% reduction in total glutathione content of the cells. In contrast, auranofin treatment did not modulate total glutathione levels and its effect on roGFP1 fluorescence ratio only reflects changes in glutathione redox state.

It is important to note that confounding effects on EPR signal dynamics may come from clearance of the spin probe from the region of interest [52, 53]. Although intra-tumoral injection of spin probes is invasive, it is the only possible delivery mode because of the fast kinetics of spectral changes in comparison with the speed of the spin probe redistribution after iv injection [53]. Nevertheless, intratumoral injection guarantees efficient spin probe delivery and low toxicity thanks to the low dosage. Of note, mito-tempo at a concentration of 100µM can cause disruption of the mitochondrial membrane potential, thereby decreasing oxygen consumption of tumor cells and increasing the level of oxygenation. In that case, the bioreduction of the nitroxide would be slower. However, the effect would be similar between the different conditions tested and would not affect the relative rates assessed in the current study, although we cannot exclude an underestimation of the absolute reduction rates.

A couple of studies assessed in vivo redox status in tumors implanted in the thigh of mice, in comparison with the contralateral muscle redox status [54,55]. However, few studies aimed at assessing efficacy of modulators of the tumor redox status. One such study however showed the ability of 3 carbamoyl-proxyl (3-CP), a cytosolic spin probe, to assess changes in redox status induced by BSO in RIF-1 tumors [51]. Whether the reduction rate can be tumor type-dependent has not been assessed so far, yet different redox properties have been described between less and more aggressive tumor cells [35].

Further cross-validation with alternative techniques for in vivo measurements would be required to assess the sensitivity of the EPR assay using mito-tempo. In vivo translation of the roGFP probes is more difficult, but could be considered on frozen tumor sections using transformed tumor cells expressing roGFP. Alternatively, transgenic mice expressing roGFP- have also recently been described [56,57]. The mito-TEMPO in vivo reduction rate could be compared to a recently published method, involving a different use of a nitroxide probe to assess in vivo gluthatione in tumors. Authors used a nitroxide probe consisting of two nitroxide rings bound by the S-S bond, which gives a different EPR spectrum from the typical one nitroxide triplet pattern. Hence, it was possible to follow the reaction between the probe and GSH by recording the increase of the monoradical EPR spectrum, and to assess the effect of BSO in FSaII tumors [36,53]. Finally, development of [1-^{13}C] dehydroascorbate [DHA], the oxidized form of Vitamin C, as an endogenous redox sensor for in vivo imaging using

hyperpolarized ^{13}C spectroscopy, was applied in tumor models in vivo [58,59]. Cross-validation with those two techniques would be relevant, yet keeping in mind that those probes are cytosolic and not mitochondrial.

In conclusion, this study is the first cross-validation of EPR redox nitroxide probes with sensitive roGFP probes, highlighting the ability of the mitochondrial EPR redox probe to assess changes induced by gluthatione and thioredoxin modulators in tumor cell lines. Further in vivo validation of the mito-tempo spin probe with alternative in vivo methods should be considered, yet the spin probe used in vivo in xenografts demonstrated sensitivity to the redox status modulators. The mitochondrial spin probe therefore seems to be promising for future tumor redox targeted treatment validation.

Fundings

This study was supported by grants from the Belgian National Fund for Scientific Research (F.R.S.-FNRS), the Communauté Française de Belgique (ARC) ARC 12/17-047 & ARC 14/19-058). Florian Gourgue is FRIA grant holder, J.C. Jonas is Research Director of the F.R.S.-FNRS, B.F.Jordan is Senior Research Associate of the F.R.S.-FNRS.

Conflict of interest

None

References

1. Trachootham D, Zhou Y, Zhang H, et al. Selective killing of oncogenically transformed cells through a ROS-mediated mechanism by beta-phenylethyl isothiocyanate. Cancer Cell. 2006;10(3):241-52.
2. DeNicola GM, Karreth FA, Humpton TJ, et al. Oncogene-induced Nrf2 transcription promotes ROS detoxification and tumorigenesis. Nature. 2011;475(7354):106-9.
3. Diehn M, Cho RW, Lobo NA, et al. Association of reactive oxygen species levels and radioresistance in cancer stem cells. Nature. 2009; 9;458(7239):780-3.
4. Balendiran GK, Dabur R, Fraser D. The role of glutathione in cancer. Cell Biochem Funct. 2004;22(6):343-52.
5. Ballatori N, Krance SM, Notenboom S, et al. Glutathione dysregulation and the etiology and progression of human diseases. Biol Chem. 2009;390(3):191-214.
6. Lisbôa da Motta L, Müller CB, De Bastiani MA, et al. Imbalance in redox status is associated with tumor aggressiveness and poor outcome in lung adenocarcinoma patients. J Cancer Res Clin Oncol. 2014;140(3):461-70.

7. Tsujikawa T, Asahi S, Oh M, et al. Assessment of the Tumor Redox Status in Head and Neck Cancer by 62Cu-ATSM PET. PLoS One. 2016;11(5):e0155635.
8. Dequanter D, Dok R, Nuyts S. Onco Targets Ther. Basal oxidative stress ratio of head and neck squamous cell carcinomas correlates with nodal metastatic spread in patients under therapy. 2017;10:259-263.
9. Bhatia M, McGrath KL, Di Trapani G, et al. The thioredoxin system in breast cancer cell invasion and migration. Redox Biol. 2016;8:68-78.
10. Kakolyris S, Giatromanolaki A, Koukourakis M, et al. Thioredoxin expression is associated with lymph node status and prognosis in early operable non-small cell lung cancer. Clin Cancer Res. 2001;7(10):3087-91.
11. Raffel J, Bhattacharyya AK, Gallegos A, et al. Increased expression of thioredoxin-1 in human colorectal cancer is associated with decreased patient survival. J Lab Clin Med. 2003;142(1):46-51.
12. Harris IS, Treloar AE, Inoue S, et al. Glutathione and thioredoxin antioxidant pathways synergize to drive cancer initiation and progression. Cancer Cell. 2015;27(2):211-22.
13. Montero AJ, Jassem J. Cellular redox pathways as a therapeutic target in the treatment of cancer.Drugs. 2011;71(11):1385-96.
14. Cohen SJ, Zalupski MM, Conkling P, et al. A Phase 2 Randomized, Double-Blind, Multicenter Trial of Imexon Plus Gemcitabine Versus Gemcitabine Plus Placebo in Patients With Metastatic Chemotherapy-naïve Pancreatic Adenocarcinoma. Am J Clin Oncol. 2015.
15. Mitchell JB, Russo A. The role of glutathione in radiation and drug induced cytotoxicity. Br J Cancer Suppl. 1987 ; 8 :96-104.
16. Biaglow JE, Lee I, Donahue J, et al. Glutathione depletion or radiation treatment alters respiration and induces apoptosis in R3230Ac mammary carcinoma. Adv Exp Med Biol. 2003;530:153-64.
17. Villablanca JG, Volchenboum SL, Cho H, et al. A Phase I New Approaches to Neuroblastoma Therapy Study of Buthionine Sulfoximine and Melphalan With Autologous Stem Cells for Recurrent/Refractory High-Risk Neuroblastoma. Pediatr Blood Cancer. 2016;63(8):1349-56.
18. O'Dwyer PJ, Hamilton TC, LaCreta FP, et al. Phase I trial of buthionine sulfoximine in combination with melphalan in patients with cancer. J Clin Oncol. 1996; 14(1):249-56.
19. Gallo JM, Brennan J, Hamilton TC, et al. Time-dependent pharmacodynamic models in cancer chemotherapy: population pharmacodynamic model for glutathione depletion following modulation by buthionine sulfoximine (BSO) in a Phase I trial of melphalan and BSO.Cancer Res. 1995 ; 15;55(20):4507-11.
20. Anderson CP, Matthay KK, Perentesis JP, et al. Pilot study of intravenous melphalan combined with continuous infusion L-S,R-buthionine sulfoximine for children with recurrent neuroblastoma. Pediatr Blood Cancer. 2015;62(10):1739-46.
21. Lun X, Wells JC, Grinshtein N, et al. Disulfiram when Combined with Copper Enhances the Therapeutic Effects of Temozolomide for the Treatment of Glioblastoma. Clin Cancer Res. 2016;22(15):3860-75.
22. Triscott J, Rose Pambid M, Dunn SE. Concise review: bullseye: targeting cancer stem cells to improve the treatment of gliomas by repurposing disulfiram. Stem Cells. 2015;33(4):1042-6.

23. Bista R, Lee DW, Pepper OB, et al. Disulfiram overcomes bortezomib and cytarabine resistance in Down-syndrome-associated acute myeloid leukemia cells.J Exp Clin Cancer Res. 2017;36(1):22.
24. Najlah M, Ahmed Z, Iqbal M, et al. Development and characterisation of disulfiram-loaded PLGA nanoparticles for the treatment of non-small cell lung cancer. Eur J Pharm Biopharm. 2017;112:224-233.
25. Daga M, Ullio C, Argenziano M, et al. GSH-targeted nanosponges increase doxorubicin-induced toxicity "in vitro" and "in vivo" in cancer cells with high antioxidant defenses. Free Radic Biol Med. 2016;97:24-37.
26. Ramanathan RK, Abbruzzese J, Dragovich T, et al. A randomized phase II study of PX-12, an inhibitor of thioredoxin in patients with advanced cancer of the pancreas following progression after a gemcitabine-containing combination. Cancer Chemother Pharmacol. 2011;67(3):503-9.
27. Bradley KA, Zhou T, McNall-Knapp RY, et al. Motexafin-gadolinium and involved field radiation therapy for intrinsic pontine glioma of childhood: a children's oncology group phase 2 study. Int J Radiat Oncol Biol Phys. 2013;85(1):e55-60.
28. Brachman DG, Pugh SL, Ashby LS, et al. Phase 1/2 trials of Temozolomide, Motexafin Gadolinium, and 60-Gy fractionated radiation for newly diagnosed supratentorial glioblastoma multiforme: final results of RTOG 0513. Int J Radiat Oncol Biol Phys. 2015;91(5):961-7. doi: 10.1016/j.ijrobp.2014.12.050.
29. Li H, Hu J, Wu S, et al. Auranofin-mediated inhibition of PI3K/AKT/mTOR axis and anticancer activity in non-small cell lung cancer cells. Oncotarget. 2016;7(3):3548-58.
30. Topkas E, Cai N, Cumming A, et al. Auranofin is a potent suppressor of osteosarcoma metastasis. Oncotarget. 2016;7(1):831-44.
31. You BR, Park WH. Auranofin induces mesothelioma cell death through oxidative stress and GSH depletion. Oncol Rep. 2016;35(1):546-51.
32. Celegato M, Borghese C, Casagrande N, et al. Preclinical activity of the repurposed drug auranofin in classical Hodgkin lymphoma. Blood. 2015;126(11):1394-7.
33. Swartz HM, Khan N, Khramtsov VV. Use of electron paramagnetic resonance spectroscopy to evaluate the redox state in vivo. Antioxid Redox Signal. 2007;9(10):1757-71.
34. Hyodo F, Soule BP, Matsumoto K, et al. Assessment of tissue redox status using metabolic responsive contrast agents and magnetic resonance imaging. J Pharm Pharmacol. 2008;60(8):1049-60.
35. Bakalova R, Zhelev Z, Aoki I, et al. Tissue redox activity as a hallmark of carcinogenesis: from early to terminal stages of cancer. Clin Cancer Res. 2013;19(9):2503-17.
36. Bačić G, Pavićević A, Peyrot F. In vivo evaluation of different alterations of redox status by studying pharmacokinetics of nitroxides using magnetic resonance techniques. Redox Biol. 2016;8:226-42.
37. Emoto MC, Matsuoka Y, Yamada KI, et al. Non-invasive imaging of the levels and effects of glutathione on the redox status of mouse brain using electron paramagnetic resonance imaging.Biochem Biophys Res Commun. 2017 15;485(4):802-806.
38. Iannone A., Tomasi A., Vannini V., et al. Metabolism of nitroxide spin labels in subcellular fraction of rat liver: I. Reduction by microsomes, Bio- chim. Biophys. Acta1034(1990)285–289.

39. Dooley CT, Dore TM, Hanson GT, et al. Imaging dynamic redox changes in mammalian cells with green fluorescent protein indicators. J Biol Chem. 2004;279(21):22284-93.
40. Roma LP, Duprez J, Takahashi HK, et al. Dynamic measurements of mitochondrial hydrogen peroxide concentration and glutathione redox state in rat pancreatic β-cells using ratiometric fluorescent proteins: confounding effects of pH with HyPer but not roGFP1.Biochem J. 2012;441(3):971-8.
41. de Souza AH, Santos LR, Roma LP, et al. NADPH oxidase-2 does not contribute to β-cell glucotoxicity in cultured pancreatic islets from C57BL/6J mice. Mol Cell Endocrinol. 2017;439:354-362.
42. Tietze F. Enzymic method for quantitative determination of nanogram amounts of total and oxidized glutathione: applications to mammalian blood and other tissues. Anal Biochem. 1969;27(3):502-22.
43. Griffith OW. Determination of glutathione and glutathione disulfide using glutathione reductase and 2-vinylpyridine. Anal Biochem. 1980;106(1):207-12.
44. Garcia J, Han D, Sancheti H, Yap LP, Kaplowitz N, Cadenas E. Regulation of mitochondrial glutathione redox status and protein glutathionylation by respiratory substrates. J Biol Chem. 2010;285(51):39646-54.
45. Hu J, Dong L, Outten CE.The redox environment in the mitochondrial intermembrane space is maintained separately from the cytosol and matrix. J Biol Chem. 2008; 283(43):29126-34.
46. Østergaard H, Tachibana C, Winther JR. Monitoring disulfide bond formation in the eukaryotic cytosol. J Cell Biol. 2004;166(3):337-45.
47. Kolossov VL, Hanafin WP, Beaudoin JN, et al. Exp Biol Med (Maywood). 2014 Inhibition of glutathione synthesis distinctly alters mitochondrial and cytosolic redox poise. 239(4):394-403.
48. Bhatia M, McGrath KL, Di Trapani G, et al. The thioredoxin system in breast cancer cell invasion and migration. Redox Biol. 2016; 8:68-78.
49. Rodman SN, Spence JM, Ronnfeldt TJ, Zhu Y, Solst SR, O'Neill RA, Allen BG, Guan X, Spitz DR, Fath MA.Enhancement of Radiation Response in Breast Cancer Stem Cells by Inhibition of Thioredoxin- and Glutathione-Dependent Metabolism. Radiat Res. 2016;186(4):385-395.
50. Kim NH, Park HJ, Oh MK, et al. Antiproliferative effect of gold(I) compound auranofin through inhibition of STAT3 and telomerase activity in MDA-MB 231 human breast cancer cells. BMB Rep. 2013;46(1):59-64.
51. Meyer AJ, Dick TP. Fluorescent protein-based redox probes. Antiox. Redox. Signal. 13(5):621-50.
52. Gallez B, Bacic G, Goda F, et al. Use of nitroxides for assessing perfusion, oxygenation, and viability of tissues: in vivo EPR and MRI studies. Magn Reson Med. 1996;35(1):97-106.
53. Epel B, Sundramoorthy SV, Krzykawska-Serda M, et al. Imaging thiol redox status in murine tumors in vivo with rapid-scan electron paramagnetic resonance. J Magn Reson. 2017;276:31-36.
54. Kuppusamy P, Li H, Ilangovan G, et al. Noninvasive imaging of tumor redox status and its modification by tissue glutathione levels. Cancer Res. 2002;62(1):307-12.
55. Ilangovan G, Li H, Zweier JL, et al. In vivo measurement of regional oxygenation and imaging of redox status in RIF-1 murine tumor: effect of carbogen-breathing. Magn Reson Med. 2002;48(4):723-30.

56. Wolf AM, Nishimaki K, Kamimura N, et al. Real-time monitoring of oxidative stress in live mouse skin. J Invest Dermatol. 2014;134(6):1701-9.
57. Wagener KC, Kolbrink B, Dietrich K, et al. Redox Indicator Mice Stably Expressing Genetically Encoded Neuronal roGFP: Versatile Tools to Decipher Subcellular Redox Dynamics in Neuropathophysiology. Antioxid Redox Signal. 2016;25(1):41-58.
58. Bohndiek SE, Kettunen MI, Hu DE, et al. Hyperpolarized [1-13C]-ascorbic and dehydroascorbic acid: vitamin C as a probe for imaging redox status in vivo. J Am Chem Soc. 2011;133(30):11795-801.
59. Keshari KR, Sai V, Wang ZJ, et al. Hyperpolarized [1-13C]dehydroascorbate MR spectroscopy in a murine model of prostate cancer: comparison with 18F-FDG PET. J Nucl Med. 2013;54(6):922-8.

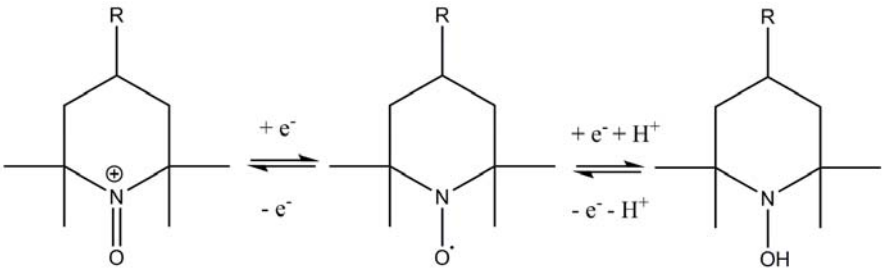

Oxoammonium — Nitroxide — Hydroxylamine

Diamagnetic — Paramagnetic — Diamagnetic

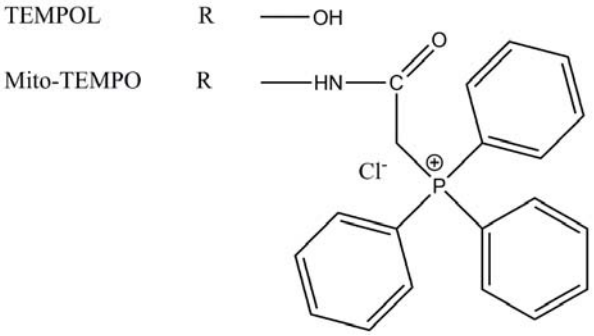

Fig.2

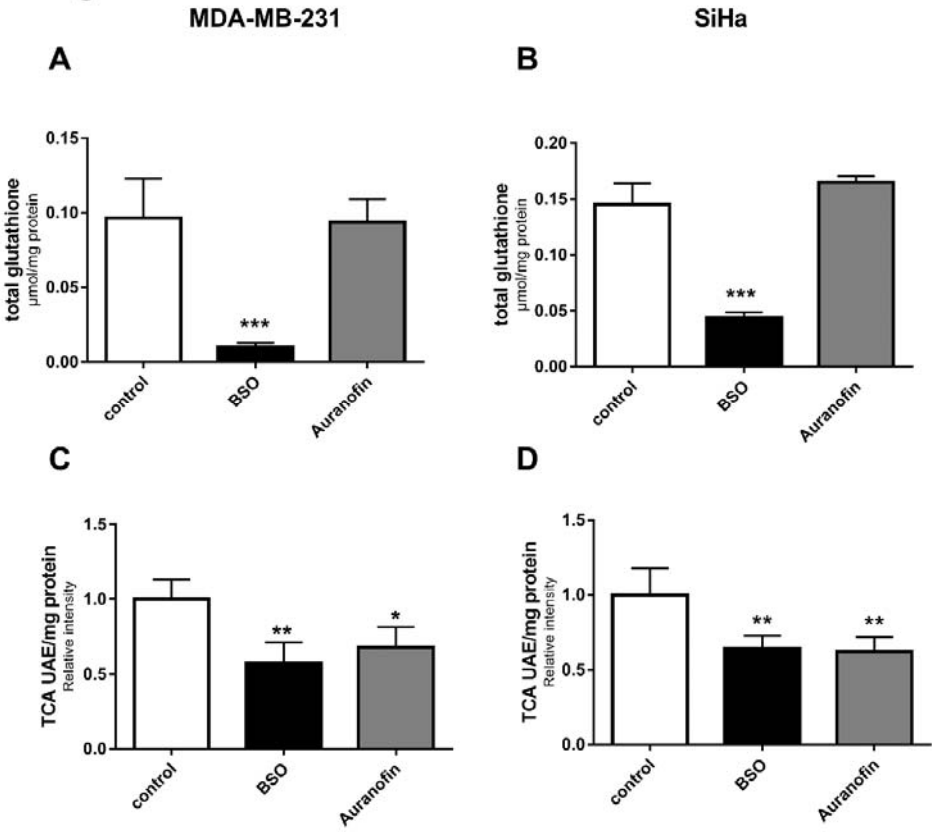

Fig.3

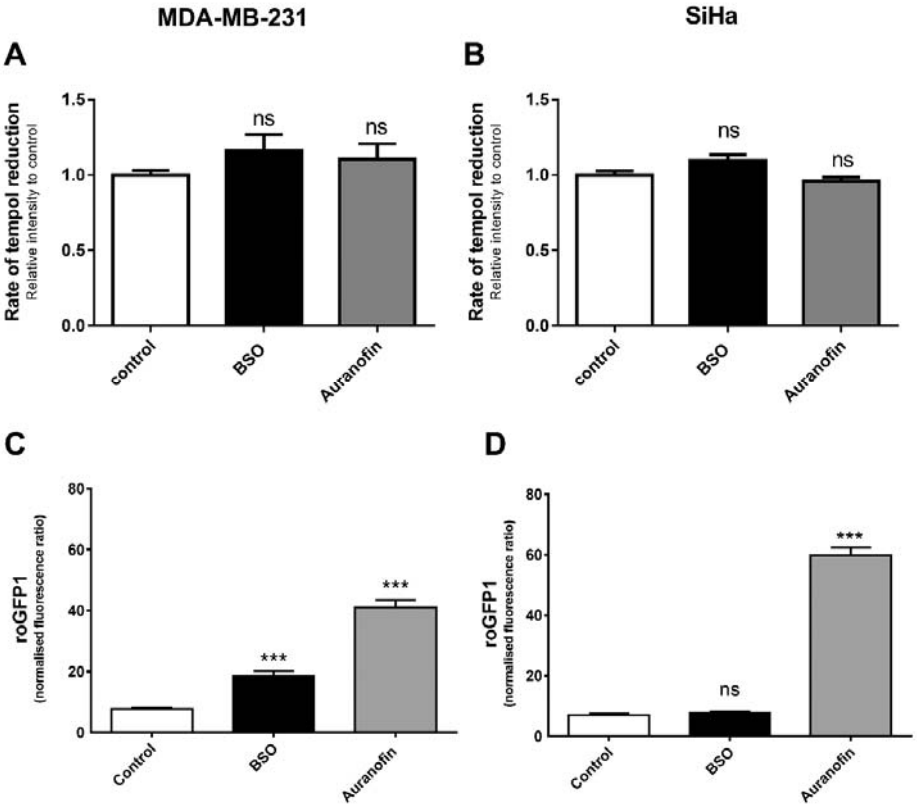
MDA-MB-231
SiHa
A
B
Rate of tempol reduction
Relative intensity to control
1.5
1.0
0.5
0.0
ns
ns
ns
ns
control
BSO
Auranofin
C
D
roGFP1
(normalised fluorescence ratio)
80
60
40
20
0
***
***
***
ns
Control
BSO
Auranofin

Fig.4

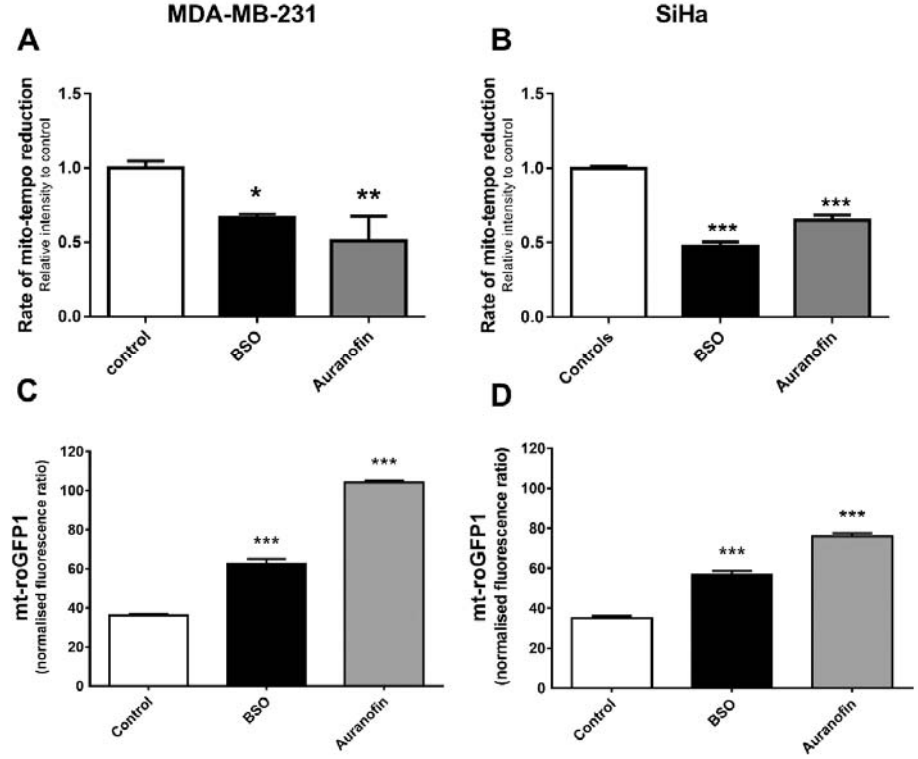
MDA-MB-231
SiHa
A
B
Rate of mito-tempo reduction
Relative intensity to control
1.5
1.0
0.5
0.0
*
**
***
***
control
Controls
BSO
Auranofin
C
D
mt-roGFP1
(normalised fluorescence ratio)
120
100
80
60
40
20
0
***
***
***
***
Control
BSO
Auranofin

Fig.5

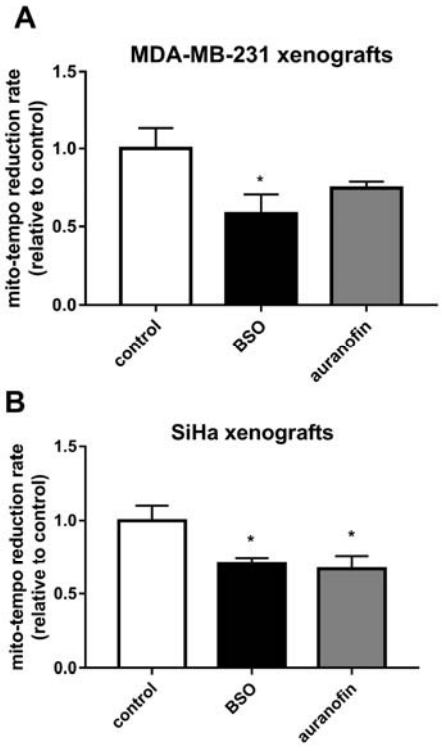
A
MDA-MB-231 xenografts
mito-tempo reduction rate (relative to control)
1.5
1.0
0.5
0.0
*
control
BSO
auranofin
B
SiHa xenografts
mito-tempo reduction rate (relative to control)
1.5
1.0
0.5
0.0
*
*
control
BSO
auranofin